Available online at www.sciencedirect.com
ScienceDirect
Trans. Nonferrous Met. Soc. China 25(2015) 2188−2194
Transactions of Nonferrous Metals Society of China
www.tnmsc.cn

Deformation mechanisms of Mg−3Al−1Zn alloy by polycrystal plasticity modeling

De-liang YIN, Jin-qiang LIU, Bing WU

School of Materials Science and Engineering, Nanjing University of Science and Technology, Nanjing 210094, China

Received 2 September 2014; accepted 25 March 2015

Abstract: A polycrystal plasticity model was developed to analyze the room-temperature deformation behaviors of Mg−3Al−1Zn alloy (AZ31). The uniaxial tension and compression tests at room temperature were conducted using cast and extruded AZ31 rods with different textures and combined with the proposed model to reveal the deformation mechanisms. It is shown that, different flow curves of two specimens under tension and compression tests can be simulated by this model. The flow curves of AZ31 extrusions exhibit different shapes for tension and compression due to different activities of tensile twinning and pyramidal ⟨*c*+*a*⟩ slip. The metallographic and TEM observations showed the equal twinning activities at the initial stage in tension and compression tests and the occurrence of pyramidal ⟨*c*+*a*⟩ slip in compression of as-cast Mg−3Al−1Zn alloy with increasing the strain, which is consistent with the simulated results by the proposed model.

Key words: Mg alloy; deformation mechanism; polycrystal plasticity model; texture

1 Introduction

Mg and its alloys usually show low ductility at ambient temperature [1−3]. Researches have proved that the ductility of Mg alloys can be substantially improved by grain size reduction and texture softening [4−6]. For instance, an AZ31 Mg alloy was subjected to an equal channel angular pressing (ECAP) and its elongation-to-failure was enhanced to above 40% [4]. Therefore, the ductility of Mg alloy at room temperature can be substantially improved by changing the microstructure and texture to activate more deformation modes such as non-basal slips and mechanical twinning. Due to the hexagonal close-packed structure, the activation stresses of slip systems differ greatly in Mg alloys, resulting in strong basal textures in their wrought products. An investigation by KHAN et al [7] showed higher strength and *r* value (the ratio of width strain to thickness strain) along the transverse direction (TD) compared with those along the rolling direction (RD), indicating important influence of slip systems on the macroscopic strength and texture of AZ31 alloy. Moreover, twinning can impose a considerable effect on the flow behaviors of Mg alloys, as revealed in the study by JIANG et al [8].

More recently, polycrystal plasticity modeling and crystal plasticity finite-element simulation [9−13] have been applied to exploring the activities of slip and twinning systems of hexagonal close-packed Mg alloys. For example, basal slip, second-order pyramidal slip and tensile twinning were regarded as the main deformation mechanisms for textured AZ31 alloy [9]. AGNEW et al [10] showed an elastic−plastic self-consistent (EPSC) model that pyramidal ⟨*c*+*a*⟩ slip was required in simulating the flow curves of Mg alloys. CHOI et al [11,12] emphasized the importance of pyramidal ⟨*c*+*a*⟩ slip in accommodating the plastic strain in Mg alloys through a visco-plastic self-consistent model. HAMA and TAKUDA [13] further discovered the difference in the activated slip systems for uniaxial tension and biaxial tension with a crystal plasticity FE method. These findings offered valuable insight into the deformation mechanisms of various Mg alloys.

In this study, a criterion for the activation of deformation mode based on the critical resolved shear stress and Schmid factor was incorporated in a simplified crystalline plasticity model to analyze the room temperature deformation mechanisms of Mg−3Al−1Zn

Foundation item: Project (51201092) supported by the National Natural Science Foundation of China
Corresponding author: De-liang YIN; Tel: +86-25-84303983; E-mail: dlyin@njust.edu.cn
DOI: 10.1016/S1003-6326(15)63831-6

(AZ31) alloys with two different textures (i.e., randomly-textured as-cast and basal-textured extruded specimens). Then, the proposed model was employed to simulate the flow curves of as-cast and extruded specimens under uniaxial tension and compression. The deformation twins and dislocations after tension/compression were analyzed by the combination of metallographic microscopy and TEM to verify the modeling results.

2 Polycrystal plasticity modeling

Owing to the hexagonal close-packed structure, the critical resolved shear stresses (CRSSs) of different deformation modes (including dislocation glide and twinning) vary markedly in Mg alloys, which makes it difficult for these modes to operate synchronously [14,15]. This feature differs from that of cubic-structure metals which have abundant equivalent slip systems with equal initial CRSSs for several slip systems to operate simultaneously.

Therefore, it is assumed in this model that merely a slip or twinning mode can be activated within an individual grain during a loading instant, but different modes can be activated during a loading period depending on their dynamically changed CRSSs and orientation factors. To ensure the continuity among grains, the normal strain rates of all grains are assumed to be the same during the loading. Four modes were considered in this model: M1 is $\{0001\}\langle 11\bar{2}0\rangle$ basal slip, M2 is $\{10\bar{1}0\}\langle 11\bar{2}0\rangle$ prismatic slip, M3 is $\{11\bar{2}2\}\langle 11\bar{2}3\rangle$ pyramidal slip, and M4 is $\{10\bar{1}2\}\langle\bar{1}011\rangle$ twinning, which have also been adopted by CHOI et al [11] and AGNEW et al [16].

Voce hardening law was adopted to calculate the CRSS for a deformation mode Mj (j=1, 2, 3, 4) with imposed strain [16,17].

$$\tau_c^{\mathrm{M}j}=\tau_0^{\mathrm{M}j}+\tau_1^{\mathrm{M}j}\left\{1-\exp\left(-\frac{\Gamma^{\mathrm{M}j}\theta_0^{\mathrm{M}j}}{\tau_1^{\mathrm{M}j}}\right)\right\}\quad (j=1,\ 2,\ 3,\ 4)\ (1)$$

where $\tau_{\mathrm{c}}^{\mathrm{M}j}$ denotes the instantaneous CRSS of mode Mj (j=1, 2, 3, 4), $\tau_0^{\mathrm{M}j}$ is the initial CRSS, $\tau_0^{\mathrm{M}j}+\tau_1^{Mj}$ represents the final back-extrapolated CRSS, $\theta_0^{\mathrm{M}j}$ denotes the initial hardening rate, $\Gamma^{\mathrm{M}j}$ represents the accumulated shear strain. The shear strain $\Delta\gamma^{\mathrm{M}j}$ accomplished by Mj during a loading step is represented by imposed normal strain increment $\Delta\varepsilon$ and Schmid factor $m^{\mathrm{M}j}$ as follows:

$$\Delta\gamma^{\mathrm{M}j}=\frac{\Delta\varepsilon}{m^{\mathrm{M}j}}\quad (2)$$

The responded normal stress $\sigma_{ci}^{\mathrm{M}j}$ of an individual grain i (i=1, ⋯, n) along loading axis can then be expressed (note that n denotes the total number of grains in the model) by

$$\sigma_{ci}^{\mathrm{M}j}=\frac{\tau_{ci}^{\mathrm{M}j}}{m_i^{\mathrm{M}j}}\quad (3)$$

Considering the fact that a slip or twinning mode is easier to operate under the conditions of low CRSS and high orientation factor, both the CRSS and Schmid factor should be incorporated into the plasticity modeling to identify which mode will be preferentially active in a single grain.

The required longitudinal stress of deformation mode Mj for grain i, $\sigma_{ci}^{\mathrm{M}j}$ (equal to $\tau_{ci}^{\mathrm{M}j}/m_i^{\mathrm{M}j}$ in Eq. (3), termed relative CRSS), can be used to embody the combined effects of CRSS and orientation factor. Hence, a criterion is proposed that the only activated mode Mj* in one grain must have the minimum value of $\sigma_{ci}^{\mathrm{M}j}$ among all the modes. Then, the activated deformation mode Mj* in grain i can be identified by calculating the minimum value among the relative CRSSs of the four involved modes.

$$\sigma_{ci}^{\mathrm{M}j^*}=\min(\sigma_{ci}^{\mathrm{M1}},\sigma_{ci}^{\mathrm{M2}},\sigma_{ci}^{\mathrm{M3}},\sigma_{ci}^{\mathrm{M4}})\quad (4)$$

For example, if the relative CRSS $\sigma_{ci}^{\mathrm{M2}}$ of $\{10\bar{1}0\}\langle 11\bar{2}0\rangle$ prismatic slip of grain i is minimum, then j*=2. The instantaneous macroscopic stress σ for a given macroscopic strain increment $\Delta\varepsilon$ can be calculated by adding up $\sigma_{ci}^{\mathrm{M}j^*}$ of all grains.

$$\sigma=\sum_{i=1}^{n}\sigma_{ci}^{\mathrm{M}j^*}=\sum_{i=1}^{n}\frac{\tau_{ci}^{\mathrm{M}j^*}}{m_i^{\mathrm{M}j^*}}\quad (5)$$

Due to the strain hardening and grain rotations, $\tau_{ci}^{\mathrm{M}j}$ of the activated mode Mj will rise, causing it more difficult to operate. As a result, other originally softer modes will be activated and contribute to the imposed normal strain increment.

The relative activity (RA) of a deformation mode Mj is calculated to analyze its contribution to plastic deformation and defined by

$$\mathrm{RA}=\frac{n_{\mathrm{M}j}}{n_{\mathrm{total}}}\quad (6)$$

where $n_{\mathrm{M}j}$ denotes the number of grains which deform by mode Mj, and n_{total} is the total number of grains used for the modeling. The RA of mode Mj embodies practically the independent contribution of this mode to the macroscopic normal strain increment $\Delta\varepsilon$ for a deformation instant in $n_{\mathrm{M}j}$ grains. Based on the above assumptions and equations, a polycrystal plasticity model considering polar nature of twinning and grain rotations was developed using Matlab 7. The orientation angles of grains in two types of textures (as-cast rods with random orientations and extruded rods with fiber basal texture) were imported to this program to simulate the deformation behavior and reveal the activities of

different modes. The parameters for this model were determined by the nonlinear fitting (based on Voce law) of the stress−strain curves of AZ31 extrusions under uniaxial tension and compression. The obtained fitting parameters are listed in Table 1, in which the negative value of τ_1 for twinning is used to describe the sigmoidal shape of twinning-dominated flow.

Table 1 Voce parameters for different deformation modes used in model

Mode	Voce parameter/MPa		
	τ_0	τ_1	θ_0
M1	25.0	90.0	250.0
M2	45.0	110.0	300.0
M3	88.0	130.0	350.0
M4	32.0	−10.0	200.0

3 Experimental

3.1 Microstructures and textures characterization

A commercial AZ31 alloy in the as-cast state was selected for the investigation. The cast AZ31 alloy specimens were extruded at 250 °C with an extrusion ratio of 9 to reduce the grain size and induce a basal fiber texture. The initial cast specimens had coarser grains size of about 162.8 μm, while the prepared extruded bars showed much finer grain size of about 8.9 μm. Both microstructures are free of twins. The textures of as-cast and extruded billets obtained by X-ray diffraction are illustrated in Fig. 1. The maximum pole intensity of (0002) plane of extruded AZ31 alloy is about 70% higher than that of cast counterpart. Additionally, basal poles of grains in as-cast AZ31 alloy (Fig. 1(a)) are randomly oriented, obviously different from the basal texture in AZ31 extrusions with the basal planes of many grains oriented parallel to the extruding direction (ED), as shown in Fig. 1(b).

Circular disks were machined from deformed specimens of cast AZ31 alloy, ground to about 100 μm thickness and electro-polished for TEM observations. Two-beam diffraction condition and $\boldsymbol{g}\cdot\boldsymbol{b}=0$ criterion were used in the TEM experiment to identify dislocations with $\langle c+a\rangle$ Burgers vector.

3.2 Mechanical testing

$\{10\bar{1}2\}\langle\bar{1}011\rangle$ tensile twinning is usually activated under tension along the c axis or compression parallel to the basal planes due to its polarity [18−20]. Consequently, the selective activation of this twinning dependent on preferred orientation has been regarded as the primary reason for the tension/compression asymmetry in textured Mg alloys [21−23]. Hence, Mg alloys with different textures are expected to show texture-dependent

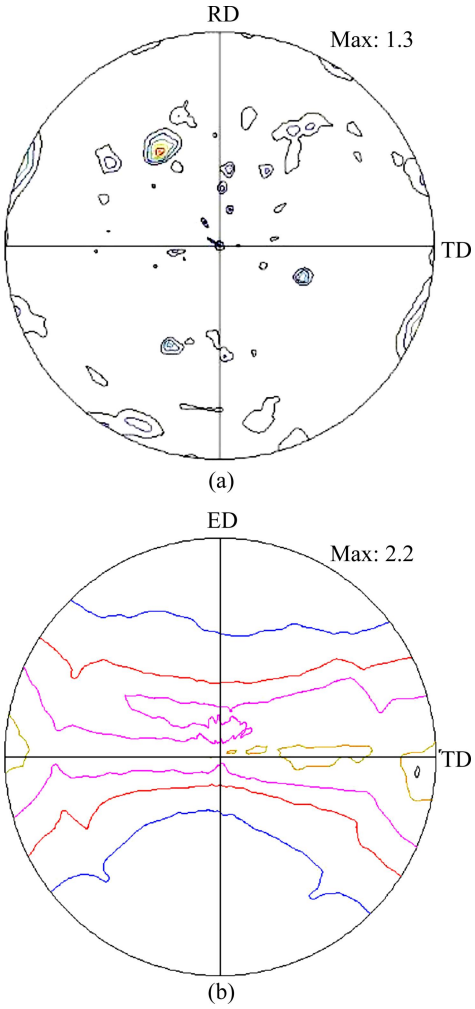

Fig. 1 (0002) pole figures showing textures of cast (a) and extruded (b) AZ31 specimens with XRD testing surface parallel to extrusion direction (ED) (TD denotes transverse direction, RD denotes radial direction of cast rods)

mechanical responses, which provide a feasible basis to acquire the fitting parameters of Voce law and develop a polycrystal plasticity model of Mg alloys.

For this purpose, AZ31 specimens with random texture (Fig. 1(a)) and fibre basal texture (Fig. 1(b)) were mechanically tested under tension and compression to obtain different plastic responses. The mechanical-test samples were cut from as-cast and extruded rods along their axes, respectively, and then deformed with a strain rate of 0.001 s^{-1} at room temperature.

4 Results and discussion

4.1 Deformation mechanisms of extruded AZ31 alloy

The experimental and modeling flow curves of extruded AZ31 alloy under uniaxial tension and compression are illustrated in Fig. 2.

The flow curves in Fig. 2 show obvious tension/compression yielding asymmetry (i.e., yielding strength

in tension is obviously higher than that in compression) and different work hardening rates. In particular, the flow curve in compression shows a concave shape and increasing work hardening rate compared with a convex shape and decreasing work hardening rate in tension. This asymmetric plastic response has been attributed to the activation of $\{10\bar{1}2\}$ tensile twinning in compression but not in tension with the presence of basal texture in extruded billets. Using the proposed model, the different tension/compression work hardening behaviors and twinning-dominated sigmoidal flow curve experimentally observed in compression are well simulated (dash lines in Fig. 2).

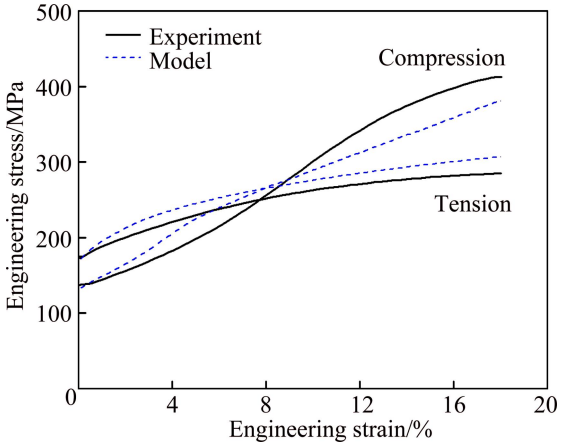

Fig. 2 Flow curves of AZ31 extrusions with basal fibre texture under tension and compression through experiments and modeling

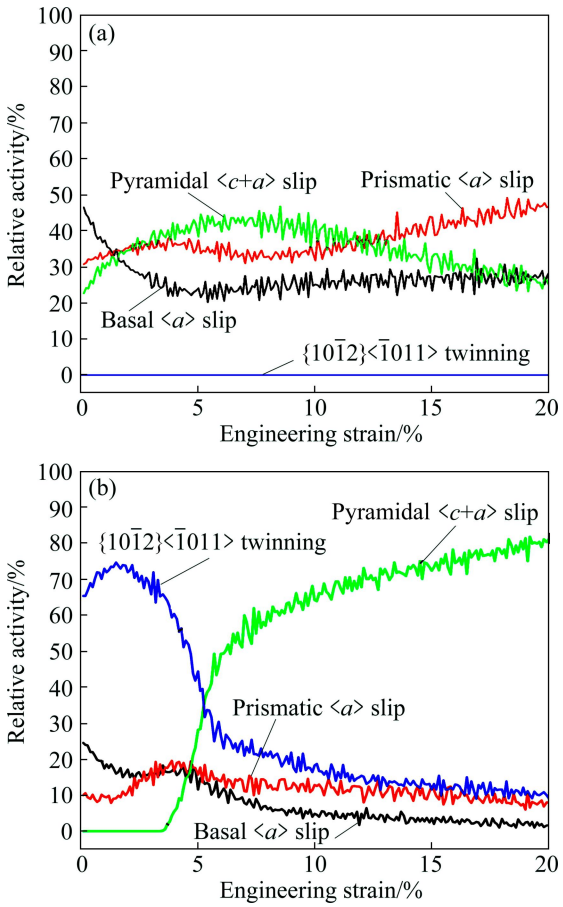

Fig. 3 Deformation mode activities under tension (a) and compression (b) for AZ31 extrusions

As shown in Fig. 3, during uniaxial tension, considerable basal $\langle a\rangle$ dislocations can be activated at the initial stage due to the not very strong basal texture. With the increase of strain and the resultant rotation of grains, the Schmid factor of activated basal $\langle a\rangle$ slip system decreases and the instantaneous CRSS becomes larger due to self-hardening. Consequently, the relative activity of basal $\langle a\rangle$ slip drops significantly to around 20% at a strain of 6%, and the hard pyramidal $\langle c+a\rangle$ slip is more favorable to operate and carry 40% deformation at a strain of 9%. Because of the basal texture in AZ31 extrusions, almost no activation of $\{10\bar{1}2\}$ twinning occurs during tension.

It should be noted that, even if a few grains are oriented away from the extruded basal texture, $\{10\bar{1}2\}$ twinning systems in these grains are still hard to activate due to their low CRSSs compared with those of basal $\langle a\rangle$ slip systems [23].

For uniaxial compression, twinning plays an important role (nearly 65%) at the initial stage, and then decreases to only 15% at a strain of 20%. In contrast, the hard pyramidal $\langle c+a\rangle$ slip begins to operate at a strain of 4% and becomes more important with increasing the strain. Since $\{10\bar{1}2\}$ twinning and pyramidal slip are the only two modes to accommodate strains along the c-axis, the increased relative activity of pyramidal slip is almost equal to the decreased activity of $\{10\bar{1}2\}$ twinning. Compared Fig. 3(a) with Fig. 3(b), obviously different activities of pyramidal slip can be understood as a result of different twinning activities in tension and compression for deformation compatibility, and also cause high strain hardening rate in compression. The relative activities of tensile twinning and pyramidal slip in tension and compression coincide with the results reported by CHOI et al [11].

4.2 Deformation mechanisms of cast AZ31 alloy

To analyze the effect of texture on the deformation mechanisms, the cast AZ31 alloy with randomly oriented grains was examined by uniaxial mechanical tests to compare with the plastic behavior of AZ31 extrusions. It can be found in Fig. 4 that, the yield strengths for tension and compression are nearly the same at the beginning of deformation. However, the work hardening rate is much higher in compression than that in tension, causing a gap of 100 MPa in flow stress. Unlike the concave curve in compression and convex curve in tension for extruded

AZ31 alloy (Fig. 2), the flow curve shapes of both tension and compression are convex for cast AZ31 alloy, implying different deformation mechanisms compared with AZ31 extrusions.

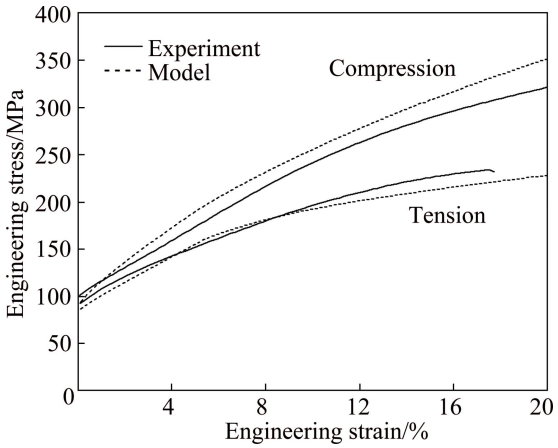

Fig. 4 Flow curves of randomly-textured cast AZ31 alloy by experiments and modeling

MANN et al [24] have demonstrated that, in cast Mg alloys with random texture, the number of favorably-oriented grains for twinning in compression is more than that in tension, and the twin growth is more pronounced. Therefore, the flow curve in compression should be lower than that in tension. However, the compression curves of both this work and CAPEK et al's work [25] overtop the tension curves for cast Mg alloys, i.e., the result contradicts to what is expected. It is noticed that the flow curves of cast Mg alloys in tension and compression showed no signature of sigmoidal shape, quite different from those of Mg extrusions. This implies that $\{10\bar{1}2\}$ extension twinning is not the predominant deformation mechanism in randomly-textured cast Mg alloys. On the other hand, there are far more grains favorably oriented for basal slip in randomly-textured cast Mg alloys than those in Mg alloy extrusions, and the basal slip will become the predominant mechanism both in tension and compression due to the much lower CRSS of basal slip than that of extension twinning. Consequently, the limited activation of twinning in cast Mg alloys cannot dominate the plastic deformation and result in a sigmoidal flow curve and a lower stress in compression than that in tension.

To account for this phenomenon quantitatively, the activities of slip and twinning in randomly-textured cast AZ31 specimens were investigated through plasticity modeling, which revealed that the predominant modes were basal slip and tensile twinning. The activities of basal slip and twinning are almost identical at the early deformation stage (Fig. 5). Therefore, the difference in yield strength between tension and compression should be small for cast AZ31 Mg alloy. These modeled results about twinning after yielding are verified by the nearly identical number of twined grains after 2% strain in tension (Fig. 6(a)) and compression (Fig. 6(b)).

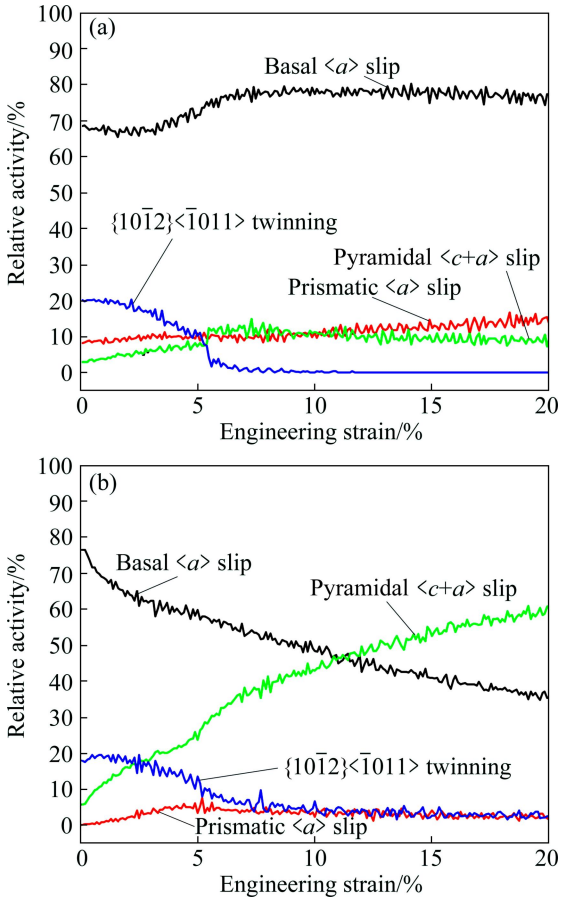

Fig. 5 Deformation mode activities under tension (a) and compression (b) for cast AZ31 alloy

Because of the low activity of pyramidal $\langle c+a\rangle$ slip to accommodate c-axis strain during tension (Fig. 5(a)), the maximum strain under tension is much smaller than that under compression. It is also implied in Fig. 5 that, the work hardening rate in compression is higher than that in tension owing to the more activities of harder pyramidal $\langle c+a\rangle$ slip in cast AZ31 alloy. To verify the occurrence of $\langle c+a\rangle$ slip on pyramidal planes of randomly-textured AZ31 alloy under compression, the dislocations were observed by TEM with vector $\boldsymbol{g}$ of [0002] after an imposed strain of 20% (Fig. 7).

Besides the dislocations with $\langle a\rangle$ Burges vector in basal plane and prismatic plane, several $\langle c+a\rangle$ dislocation segments can be found with their directions neither parallel nor perpendicular to (0001) trace line. This observation agrees with the theoretical study by YOO et al [26], which shows that $\langle c+a\rangle$ dislocations can form under relatively large driving forces provided by activated prismatic slip of $\{10\bar{1}0\}\langle 11\bar{2}0\rangle$ dislocations. These dislocation lines with $\langle c+a\rangle$ Burgers vector present a direct evidence for the activation of pyramidal $\langle c+a\rangle$

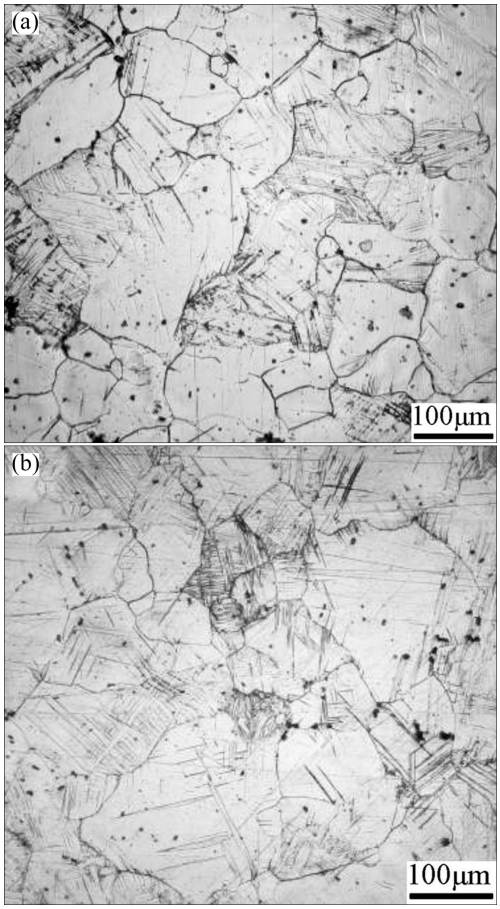

Fig. 6 Metallographic photographs of cast AZ31 alloy under tension (a) and compression (b) after 2% strain

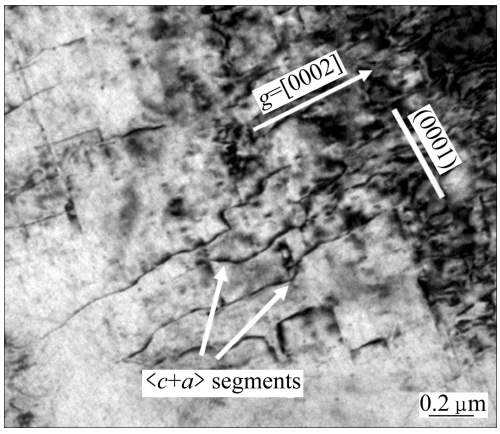

Fig. 7 Pyramidal ⟨*c*+*a*⟩ dislocations in compressed cast AZ31 alloy after 20% strain by TEM

slip and should be an important reason for different work hardening behaviors of as-cast specimens.

5 Conclusions

1) The flow curves of AZ31 extrusions exhibit concave shape for compression and convex shape for tension due to significantly different activities of $\{10\bar{1}2\}$ twinning, while the flow curves of cast AZ31 alloy show identical convex shapes but different work hardening rates as a result of different activities of pyramidal ⟨*c*+*a*⟩ slip.

2) The number of grains undergoing twinning after yielding under tension and compression in cast AZ31 alloy are nearly the same in optical micrographs, which is consistent with the simulated relative activity of $\{10\bar{1}2\}$ twinning by the model.

3) The TEM micrographs show the ⟨*c*+*a*⟩ dislocation segments in cast AZ31 alloy compressed to 20% strain, confirming the activity of pyramidal ⟨*c*+*a*⟩ slip and its different roles in work hardening of cast AZ31 alloy under tension and compression.

References

[1] AVEDESIAN M M, BAKER H. ASM specialty handbook: Magnesium and magnesium alloys [M]. Ohio: ASM International, 1999: 168.

[2] GU C F, TOTH L S, FIELD D P, FUNDENBERGER J J, ZHANG Y D. Room temperature equal-channel angular pressing of a magnesium alloy [J]. Acta Materialia, 2013, 61(8): 3027−3036.

[3] WANG Li-fei, HUANG Guang-sheng, LI Hong-cheng, ZHANG Hua. Influence of strain rate on microstructure and formability of AZ31B magnesium alloy sheets [J]. Transactions of Nonferrous Metals Society of China, 2013, 23(4): 916−922.

[4] MUKAI T, YAMANOI M, WATANABE H. Ductility enhancement in AZ31 magnesium alloy by controlling its grain structure [J]. Scripta Materialia, 2001, 45(1): 89−95.

[5] KOIKE J, KOBAYASHI T, MUKAI T. The activity of non-basal slip systems and dynamic recovery at room temperature in fine-grained AZ31B magnesium alloys [J]. Acta Materialia, 2003, 51(7): 2055−2065.

[6] CHEN Yong-jun, WANG Qu-dong, LIN Jin-bao, LIU Man-ping. Grain refinement of magnesium alloys processed by severe plastic deformation [J]. Transactions of Nonferrous Metals Society of China, 2014, 24(12): 3747−3754.

[7] KHAN A S, PANDEY A, THOMAS G H, MISHRA R K. Mechanical response and texture evolution of AZ31 alloy at large strains for different strain rates and temperatures [J]. International Journal of Plasticity, 2011, 27(5): 688−706.

[8] JIANG J, JONAS J J, MISHRA R K, LUO A A, SACHDEV A K, GODET S. Twinning and texture development in two Mg alloys subjected to loading along three different strain paths [J]. Acta Materialia, 2007, 55(11): 3899−3910.

[9] STAROSELSKY A, ANAND L. A constitutive model for HCP materials deforming by slip and twinning: Application to magnesium alloy AZ31B [J]. International Journal of Plasticity, 2003, 19(10): 1843−1864.

[10] AGNEW S R, BROWN D W, TOMÉ C N. Validating a polycrystal model for the elastoplastic response of magnesium alloy AZ31 using in situ neutron diffraction [J]. Acta Materialia, 2006, 54(18): 4841−4852.

[11] CHOI S H, SHIN E J, SEONG B S. Simulation of deformation twins and deformation texture in an AZ31 Mg alloy under uniaxial compression [J]. Acta Materialia, 2007, 55(12): 4181−4192.

[12] CHOI S H, KIM D W, SEONG B S, ROLLETT A D. 3-D simulation of spatial stress distribution in an AZ31 Mg alloy sheet under in-plane compression [J]. International Journal of Plasticity, 2011, 27(10): 1702−1720.

[13] HAMA T, TAKUDA H. Crystal plasticity finite-element simulation of work-hardening behavior in a magnesium alloy sheet under biaxial tension [J]. Computational Materials Science, 2012, 51(1): 156−164.
[14] LOU X Y, LI M, BOGER R K. Hardening evolution of AZ31B Mg sheet [J]. International Journal of Plasticity, 2007, 23(1): 44−86.
[15] BARNETT M R, KESHAVARZ Z, MA X. A semianalytical Sachs model for the flow stress of a magnesium alloy [J]. Matallurgical and Materials Transactions A, 2006, 37(7): 2283−2293.
[16] AGNEW S R, TOMÉ C N, BROWN D W. Study of slip mechanisms in a magnesium alloy by neutron diffraction and modeling [J]. Scripta Materialia, 2003, 48(8): 1003−1008.
[17] PROUST G, TOMÉ C N, KASCHNER G C. Modeling texture, twinning and hardening evolution during deformation of hexagonal materials [J]. Acta Materialia, 2007, 55(6): 2137−2148.
[18] CHRISTIAN J W, MAHAJAN S. Deformation twinning [J]. Progress in Materials Science, 1995, 39(1−2): 1−157.
[19] GODET S, JIANG L, LUO A A, JONAS J J. Use of Schmid factors to select extension twin variants in extruded magnesium alloy tubes [J]. Scripta Materialia, 2006, 55(11): 1055−1058.
[20] BROWN D W, AGNEW S R. Internal strain and texture evolution during deformation twinning in magnesium [J]. Materials Science and Engineering A, 2005, 399(1−2): 1−12.
[21] KLEINER S, UGGOWITZER P J. Mechanical anisotropy of extruded Mg−6%Al−1%Zn alloy [J]. Materials Science and Engineering A, 2004, 379(1−2): 258−263.
[22] WANG Jing-tao, YIN De-liang, LIU Jin-qiang. Effect of grain size on mechanical property of Mg−3Al−1Zn alloy [J]. Scripta Materialia, 2008, 59(1): 63−66.
[23] YIN De-liang, WANG Jing-tao, LIU Jin-qiang, ZHAO Xiang. On tension−compression yielding asymmetry in an extruded Mg−3Al−1Zn alloy [J]. Journal of Alloys and Compounds, 2009, 478(1−2): 789−795.
[24] MANN G E, SUMITOMO T, CÁCERES C H, GRIFFITHS J R. Reversible plastic strain during cyclic loading-unloading of Mg and Mg−Zn alloys [J]. Materials Science and Engineering A, 2007, 456(1−2): 138−146.
[25] ČAPEK J, MÁTHIS K, CLAUSEN B, STRÁSKÁ J, BERAN P, LUKÁŠ P. Study of the loading mode dependence of the twinning in random textured cast magnesium by acoustic emission and neutron diffraction methods [J]. Materials Science and Engineering A, 2014, 602: 25−32.
[26] YOO M H, AGNEW S R, MORRIS J R, HO K M. Non-basal slip systems in HCP metals and alloys: Source mechanisms [J]. Materials Science and Engineering A, 2001, 319−321: 87−92.

采用多晶塑性模型研究 Mg−3Al−1Zn 合金的变形机制

尹德良，刘金强，吴 冰

南京理工大学 材料科学与工程学院，南京 210094

摘 要：采用一种多晶塑性模型分析 Mg−3Al−1Zn 合金的室温变形行为。使用铸态和挤压态两种织构类型的 AZ31 镁合金棒料进行室温单向拉伸和压缩试验，并与提出的模型相结合来揭示该合金的变形机制。结果表明：多晶塑性模型可以成功地模拟镁合金试样拉伸和压缩曲线的差异。挤压态 AZ31 镁合金拉伸和压缩曲线形状的差异是拉伸孪生和锥面⟨*c*+*a*⟩滑移的不同开动行为所致。金相和透射电镜(TEM)观察表明：铸态 AZ31 镁合金拉伸和压缩初期具有相同的孪生开动分数；随着应变的增加，在铸态压缩试样中发生了锥面⟨*c*+*a*⟩滑移，这与模拟结果相吻合。

关键词：镁合金；变形机制；多晶塑性模型；织构

(Edited by Mu-lan QIN)